Talanta 288 (2025) 127729

Contents lists available at ScienceDirect

Talanta

journal homepage: www.elsevier.com/locate/talanta

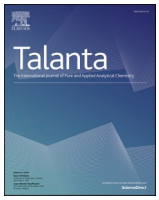

Comparative electrochemical study of oxidative nicarbazin determination in non-aqueous media: Differential pulse voltammetry vs. capillary electrophoresis with amperometric detection

Sofiia Ivakh [a,1], Martin Koall [b,1], Jiří Barek [a], Frank-Michael Matysik [b,*]

[a] Charles University, Faculty of Science, Department of Analytical Chemistry, UNESCO Laboratory of Environmental Electrochemistry, Hlavova 8, Prague 2, 128 00, Czech Republic
[b] Institute of Analytical Chemistry, Chemo- and Biosensors, University of Regensburg, Universitätsstraße 31, Regensburg, 93053, Germany

ARTICLE INFO

Keywords:
Electrochemistry
Complementary study
Capillary electrophoresis
Differential pulse voltammetry
Electrochemical detection
Quality control
Mass spectrometry

ABSTRACT

Background: Electrochemistry offers a range of powerful techniques for solving analytical problems, each with its own advantages and limitations that can significantly affect the information obtained. These variations lead to diverse requirements for newly developed methods. Applying multiple electrochemical techniques simultaneously can optimize information extraction from a sample, aiding in the selection of the best analytical approach.

Results: In this study, we present the first investigation of the oxidation of the coccidiostat nicarbazin, along with a comparative evaluation of two established electrochemical methods with complementary strengths: differential pulse voltammetry (DPV) and capillary electrophoresis coupled with amperometric detection (CE-AD). We thoroughly examine the oxidative determination of nicarbazin in poultry feed samples using acetonitrile based media. DPV allows for rapid and efficient analysis, while CE-AD excels in handling complex samples with electrochemically active species due to its high separation efficiency. Both methods exhibit limits of detection (LODs) in the low micromolar range. To provide a comprehensive understanding of the nicarbazin oxidation process, the final reaction products were analyzed by mass spectrometry, identifying 4-nitroaniline and (4-nitrophenyl)formamide as key product compounds.

Significance and novelty: This pioneering research on the anodic detection of nicarbazin includes a detailed analysis of the components in the studied equimolar mixture. The developed protocols, combined with straightforward sample preparation, enable the successful determination of nicarbazin levels below those allowed by EU regulations.

1. Introduction

In the rapidly evolving field of analytical techniques for the detection of biologically active molecules and the characterization of their conversion on electrode surfaces, there is an increasing emphasis on developing more innovative and cutting-edge analytical approaches. Thus, it has become increasingly clear that progress in this field requires multifaceted strategies in which instrumental advancements are holistically interplayed with analytical and theoretical developments [1]. In this context, the concept of utilizing capillary electrophoresis hyphenated to amperometric detection (CE-AD) and differential pulse voltammetry (DPV) represents powerful analytical tools, enabling complementary investigation of the processes occurring during analyte conversion, using the unique strengths of both separation and detection techniques.

Among the variety of separation techniques, CE is an attractive method due to remarkably high separation efficiency, excellent selectivity [2,3] throughput [4,5], and low consumption of sample [4]. With the great efforts in the past decades, the coupling of CE with AD has propelled the field forward, significantly enhancing analytical capabilities by combining high-resolution separation with sensitive detection for electroactive analytes [6–8].

Regarding static monitoring, DPV has long been established as a versatile method applying voltage pulses superimposed on a linear

* Corresponding author.
E-mail address: frank-michael.matysik@chemie.uni-r.de (F.-M. Matysik).
[1] Equally contributing author.

https://doi.org/10.1016/j.talanta.2025.127729
Received 10 December 2024; Received in revised form 30 January 2025; Accepted 10 February 2025
Available online 11 February 2025

potential sweep or staircase waveform. Here, the current is sampled immediately before pulse application and at the end of the pulse. The difference between both currents is plotted as a function of potential [9,10]. The resulting measurement provides fundamental information about kinetic and thermodynamic parameters of electrochemical processes [11,12], along with extensive opportunities for practical applications across various fields such as food safety [13], environmental monitoring [14], pharmaceutical analysis [15], biochemical research [16], clinical diagnostics [17], DNA interaction studies [18,19], and material science [20]. Within the context of its many advantages, simplicity, and flexibility, easy automation can be named, making DPV suitable for a wide range of applications, from laboratory settings to field analyses.

An important aspect that improves the potential application of the aforementioned techniques is the rational choice of background electrolyte (BGE) and the material of the working electrode. Considering the properties of an ideal electrode material [21], in acetonitrile (ACN) based BGE, platinum is predominantly utilized due to its simplicity of construction, non-toxicity, relatively high chemical inertness, and stability across a wide range of temperatures, and pressures [22]. Moreover, moving toward miniaturization, the use of Pt ultramicroelectrode (Pt UME) offers potential for field analysis, requiring only a few drops of sample.

Regarding the choice of BGE, non-aqueous media are recognized as attractive alternatives to conventional aqueous buffer solutions since they provide enhanced electrochemical stability and minimize liquid junction potential, resulting in more accurate and stable measurements [23]. Among the various choices of organic solvents, ACN exhibits the largest ratio of dielectric constant to viscosity, which leads to a high electroosmotic velocity and fast CE separations [24]. Additionally, it is perfectly suitable for performing electrochemical measurements owing to the extended accessible potential range [24]. A further advantage of ACN based BGE is the enhanced solubility of hydrophobic compounds [25] and its ability to effectively address complex separation problems [26], which is crucial for the analyte of our interest – nicarbazin (NIC).

NIC is a widely used veterinary drug to avoid coccidiosis disease in poultry [27]. It consists of an equimolar mixture of two compounds: 4,4′-dinitrocarbanilide (DNC) and 2-hydroxy-4,6-dimethylpyrimidine (HDP), which undergoes fast *in vivo* dissociation into these two individual substances. The active component is DNC (hydrophobic, solubility in water is lower than 0.02 mg/L), while HDP (hydrophilic) increases DNC absorption [28]. Therefore, the effectiveness of the mixture is higher than that of DNC used alone [29].

Nowadays, coccidiosis has been estimated as a significant challenge in animal health management, causing a variety of harmful effects on domestic animal welfare, including reduced weight gain, poor feed conversion, decreased egg production in poultry, and high mortality [30], leading to profound economic implications for the agricultural industry [31]. From this point of view, the implementation of coccidiostats in animal feed has become a routine practice to treat and prevent the disease. According to Regulation (EC) No 1831/2003 [32], NIC belongs to the 11 coccidiostats approved as feed additives within the European Union, with NIC being used in more than 60 % of cases [33]. As a result, there is concern over chronic toxicity for humans due to long-term exposure to low levels of NIC presented in animal food [30]. Despite its obvious benefits to livestock management, NIC poses a threat to the safety of the breeding industry, the ecological environment, and human health. Due to this, NIC residues in poultry feed, environmental objects, and food of animal origin should be monitored.

The number of methods available for NIC monitoring is quite limited, with the most commonly employed techniques being chromatographic methods, such as liquid chromatography with various types of detectors [34–54]. Among other published approaches, enzyme-linked immunosorbent assays [55–57], surface plasmon resonance biosensor [58], and lateral flow device [59] can be named. Within electrochemical techniques, reports on the reduction of NIC on hanging mercury drop electrodes [60–62], on glassy carbon electrode modified by multiwalled carbon nanotubes and polystyrene [63], and on screen-printed carbon electrode modified by Prussian Blue cubes [64] should be mentioned. However, to the best of our knowledge, no electrochemical method has been reported for the investigation of NIC oxidation.

Drawing inspiration from the above, we have aimed to investigate NIC oxidation on Pt UME in non-aqueous media, utilizing CE-AD and DPV, addressing a previously unexplored area within the electrochemical study of NIC. While DPV determination offers advantages in terms of time efficiency, cost-effectiveness, and portability, CE-AD excels with its minimal sample consumption and exceptional separation efficiency. Moreover, products of NIC oxidation were identified and characterized by online-coupling of pre-separation electrochemistry to capillary electrophoresis hyphenated to mass spectrometry (EC-CE-MS). This report aims to fill a critical gap in the literature but also to contribute to practical applications by developing straightforward and sensitive methods for NIC monitoring in diverse feed samples, thereby enhancing food safety and animal welfare.

2. Materials and methods

2.1. Materials

Nicarbazin (NIC, CAS No. 330-95-0), 4,4′-dinitrocarbanilide (DNC, CAS No. 587-90-6), 2-hydroxy-4,6-dimethylpyrimidine (HDP, CAS No. 108-79-2), N-(4-nitrophenol)formamide (CAS No. 16135-31-2), and 4-nitroaninline (CAS No. 100-01-6) were purchased from Sigma Aldrich and used as received. Acetonitrile (ACN), ammonia (25 %), ammonium acetate, formic acid, sodium hydroxide (NaOH), and caffeine (CAF) were purchased from Merck (Darmstadt, Germany). Acetic acid and 2-propanol (LC-MS grade) were purchased from Carl Roth (Karlsruhe, Germany). Ultrapure water was provided by a Milli-Q Advantage A10 system (Merck Darmstadt, Germany). Real feed samples were provided by National Reference Laboratory of Veterinary Drug Residues Control (State Scientific Research Control Institute of Veterinary Medicinal Products and Feed Additives, Lviv, Ukraine).

Fused silica capillaries (75 μm inner diameter, 365 μm outer diameter, polyimide coated) were purchased from Polymicro Technologies (Phoenix, USA).

The BGE composition used in CE-AD was 1.0 M acetic acid and 10 mM ammonium acetate dissolved in ACN. The BGE composition used in DPV was 0.5 mM acetic acid and 5 mM ammonium acetate dissolved in ACN. The lower concentrations in DPV were chosen due to lower background currents during the measurements.

The stock solutions of NIC, DNC and HDP (0.10 mM) were prepared by dissolving the appropriate amount of the substances in ACN in 10.0 mL volumetric flask with the aid of an ultrasonic bath (5 min). All stock solutions were stored in the refrigerator at 4 °C in the dark for one week. The working and calibration solutions were prepared freshly each day by dilution of the stock solution with a selected BGE (10.0 mM ammonium acetate and 1.0 M acetic acid in ACN for CE-AD or 5.0 mM ammonium acetate and 0.5 M acetic acid in ACN for CV, DPV).

For CV, CE-MS and EC-CE-MS studies, every day freshly prepared 0.50 mM stock solutions of DNC, HDP, and NIC using ultrasonification for 15 min were used, (at this concentration, the solutions were not stable overnight).

2.2. Instrumentation and software

2.2.1. DPV and CV setup

All electrochemical experiments were carried out using a BioLogic SP-200 instrument equipped with an ultralow current module (BioLogic, Seyssinet-Pariset, France) controlled by EC-Lab V11.46 software. Voltammetric measurements were performed in a commercial 5 mL glass electrochemical cell (ALS Co., Japan). A three-electrode set-up consisted of lab-made platinum ultramicroelectrode (Pt UME, $d_{Pt} = 25$ μm, sealed

in a glass tube), lab-made silver-silver chloride electrode ($d_{Ag} = 0.5$ mm, enclosed in a glass tube with a frit submerged in BGE) and platinum wire ($d_{Pt} = 0.3$ mm, lab-made) employed as working, reference and counter electrode, respectively.

2.2.2. CE-AD setup

For CE-AD, a laboratory-made CE system [7], hyphenated to a laboratory-constructed amperometric detector cell [24], was used. Labview-based software was used to operate the CE system. Briefly, a user-friendly cell design of a three-electrode system based on two symmetrically arranged stainless steel tubes was used for AD. A 50 μm Pt disk electrode served as a working electrode, and an Ag|AgCl wire served as a reference electrode. The stainless-steel tube, which was used as capillary guiding, served as an auxiliary electrode for the AD cell and was grounded to close the CE circuit. The electrodes were positioned using an UltraZoom Pro digital microscope from dnt (Dietzenbach, Germany). The three-electrode-system was connected to a BioLogic SP-200 instrument equipped with an ultralow current module (BioLogic, Seyssinet-Pariset, France) controlled by EC-Lab V11.46 software.

The separation capillary (length: 60 cm, inner diameter 75 μm) was prepared using the following protocol: capillary tips were polished to a 90° angle. Afterward, the capillary was flushed with 0.1 M NaOH (for 10 min), followed by water (5 min), and then followed by BGE (30 min). The capillary was stored in ACN overnight.

The voltammetric and AD cells were kept in a laboratory-constructed Faraday cage to reduce electromagnetic interference effects.

2.2.3. CE-MS and EC-CE-MS setup

For the EC-CE-MS, the MINI CE system was equipped with the laboratory-constructed injection unit described in Ref. [7] and a 50 cm fused silica separation capillary with an I.D. of 75 μm. A thin-film electrode system with platinum working, counter, and pseudo-reference electrode (ED-SE1-PT, Micrux Technologies, Oviedo, Spain) was used in the injection cell for electrochemical oxidation. The electrode was connected to a μAutolab potentiostat/galvanostat (Metrohm Autolab B. V., Utrecht, Netherlands). For the CE-MS studies the injection module was replaced by a standard glass vial (ND 9, Carl Roth, Karlsruhe, Germany). A micrOTOF from Bruker Daltonics (Bremen, Germany) with a coaxial sheath liquid ESI interface from Agilent Technologies (Santa Clara, USA) was used for mass spectrometry. The device was operated with the following parameters: nebulizer gas pressure 0.3 bar, dry gas (N_2) flow 2.5 L/min, dry gas temperature 240 °C, and *m/z* 50–600. The sheath liquid had a flow rate of 480 μL/min. Data Analysis 4.0 SP1 from Bruker Daltonics (Bremen, Germany) and MZmine 3 [65] were used for data acquisition. Mass spectra were simulated with Prot pi 2.2.29.152 online tool from Prot pi (Wädenswil, Switzerland).

2.3. Experimental procedures

2.3.1. CV and DPV measurements

CV was employed for the preliminary studies of the electrochemical behavior of NIC and its respective components (HDP and DNC). DPV was applied for the development of the novel electroanalytical protocol. All measurements were carried out in triplicate for each concentration at laboratory temperature.

The general procedure to obtain voltammograms was as follows: an appropriate amount of the stock solution of the tested substance was placed in a 2.0 mL vial, and the system was filled up completely with BGE (5.0 mM ammonium acetate and 0.5 M acetic acid in ACN) to 1.0 mL. All voltammetric measurements were carried out in 1.0 mL of analyzed solution.

Parameters of DPV were set as follows: pulse height 100 mV, pulse width 100 ms, step potential 10 mV, and scan rate of 50 mV s^{-1}. In CV, the potential range from −0.2 to 1.7 V and backward with the scan rate 100 mV s^{-1} was used.

For DPV, peak height (I_p) was evaluated against the baseline, the background correction was performed using the OriginPro 2024b (Academic) software. This approach was vital for analyzing DPV recordings, as it improves the signal-to-noise ratio and enhances the accuracy of integrating signals that manifest as shoulders on the steep sides of voltammograms. Additionally, it can reduce the background current by nearly 99 %. Conversely, CV recordings in this paper are presented without any background correction.

2.3.2. CE-AD measurements

The AD cell was filled with BGE (10.0 mM ammonium acetate and 1.0 M acetic acid in ACN) before the measurements. Subsequently, the potential shift in the AD cell caused by the CE circuit was determined and compensated by the method described by Matysik [66]. Briefly, the influence of the HV (high voltage) was determined separately by CVs of the AD cell with and without HV applied, and an AD overpotential was applied. The sample was injected hydrodynamically for 10 s. The separation voltage was 20 kV. Prior to each CE-AD measurement, an electrochemical pretreatment protocol was performed: 2.5 V for 10 s followed by −0.5 V for 10 s in AD cell filled with BGE. This procedure was used to avoid fouling of the AD working electrode. Subsequently, the detection potential of 2.0 V (corrected potential in the presence of HV) was applied.

2.3.3. CE-MS and EC-CE-MS studies

CE-MS studies were performed to investigate the migration behavior of NIC, HDP, and DNC. For these studies, the micrOTOF was operated in positive ion polarity mode, and a sheath liquid based on H_2O:2-propanol:formic acid (49.95:49.95:0.1, v:v:v) was used.

For EC-CE-MS measurements, the micrOTOF was operated in negative ion polarity mode using a sheath-liquid consisting of H_2O:2-propanol:ammonia (49.975:49.975:0.05, v:v:v). NIC, DNC (0.5 mM in ACN based BGE), and pure ACN based BGE were injected from the surface of the micrux Pt thin-film electrode while a potential of 2.5 V *vs.* Pt was applied hydrodynamically for 60 s into CE. Prior to injection, the electrochemical injection module was kept at 2.5 V for 300 s. NIC, DNC (0.5 mM in ACN based BGE), and 4-nitroanline (1 mM in ACN based BGE) were also injected at open circuit potential (OCP).

2.3.4. Feed samples preparation

For the investigation of different poultry feed samples, calibration solutions of NIC from 5.0 to 75.0 μM in BGE (10.0 mM ammonium acetate and 1.0 M acetic acid in ACN for CE-AD or 5.0 mM ammonium acetate and 0.5 M acetic acid in ACN for DPV) were prepared. 1.5 g of real feed was extracted with 5 mL of pure ACN. 50 mg of real feeding premix were extracted with 20 mL of pure ACN. All extractions were carried out for 10 min using a UP50/100 ultrasonic processor from Hielscher Ultrasonics (Teltow, Germany), equipped with an MS1 sonotrode. An ice-bath was used to prevent solvent evaporation. The extract was filtered by a syringe filter (ROTILABO® 0.45 μm, PTFE, Carl Roth, Karlsruhe, Germany).

Before CE-ED and DPV analysis, the samples were diluted with BGE 1:1. For matrix-fortified calibration for DPV, the ratio between feed extract and BGE was 3:1 due to limited solubility of NIC.

3. Results and discussion

3.1. Investigation of NIC oxidation in acetonitrile based media on platinum electrodes by CV, DPV and CE-AD

3.1.1. Electrochemical study of NIC, HDP and DNC

This study presents a pioneering investigation of the electrochemical oxidation of NIC. Specifically, for the first time, the anodic behavior of the analyte on Pt UME has been explored in a non-aqueous media. Since NIC is an equimolar mixture of two compounds, the first part of the research was aimed at achieving a comprehensive understanding of the

electroanalytical responses of NIC constituents, namely DNC and HDP, which provides insights into elucidating the redox properties and possible interactions of these compounds. CV and CE-AD were employed to establish which component of the target analyte (NIC) is electroactive and/or charged.

Initially, CV of the individual components ($C_{DNC} = C_{HDP} = 450.0$ μM) was recorded from −0.2 V to 1.7 V and backwards with the scan rate of 100 mV s^{-1} in BGE (5.0 mM ammonium acetate and 0.5 M acetic acid in ACN) and compared with CV of NIC ($C_{NIC} = 450.0$ μM) recorded under identical conditions. As illustrated in Fig. 1 (right panel), a single anodic wave was observed for HDP, DNC and NIC, showing their oxidation on Pt UME begins at approximately 1.0 V. The voltammetric waves of both DNC and HDP significantly overlap with the NIC signal, this fact indicates that both constituents of the equimolar mixture are electroactive and contribute to the overall oxidation signal of NIC. On reversing the voltammetric scan no cathodic waves of NIC were observed, indicating irreversible oxidation of NIC on the Pt UME in ACN based BGE.

Additionally, CV of caffeine (CAF), ($C_{CAF} = 450.0$ μM), depicted at the bottom of the right panel of Fig. 1 demonstrates the electrochemical activity of model analyte under given conditions.

For the investigation of the migration behavior and the amperometric response of NIC and its respective components, solutions of NIC, HDP, and DNC ($C_{NIC} = C_{DNC} = C_{HDP} = 50.0$ μM) in BGE (10.0 mM ammonium acetate and 1.0 M acetic acid in ACN) were examined. CAF ($C_{CAF} = 50.0$ μM) was used as an EOF marker. The corresponding electropherograms are displayed in Fig. 1 (left panel). Here, NIC shows two distinct amperometric signals, the first at a migration time of 280 s and the second at a migration time of 380 s. A comparison with the electropherogram of HDP shows that the first signal of NIC is related to HDP. Additionally, HDP shows the same migration behavior as CAF, which is neutral in ACN based BGE, leading to the conclusion that HDP in pure form and in NIC is neutral under the given CE conditions. A comparison of the electropherograms of NIC and DNC leads to the conclusion that the second signal of NIC corresponds to DNC. This signal is located within the migration window for the negative species, suggesting that DNC is deprotonated in ACN. The DNC-related signal of the NIC electropherogram was chosen for all subsequent determinations of NIC using CE-AD as it shows a selective migration behavior and a distinct amperometric response. Additionally, the presence of two distinct amperometric signals in the electropherogram of NIC, which correspond to the respective electropherogram of DNC and HDP, suggests a dissociation of the NIC mixture in ACN based BGE.

Additional CE-MS studies were conducted (see Fig. S1) to confirm the dissociation of NIC into HDP and DNC in ACN based BGE. The results of the CE-MS experiments are summarized in Table 1.

The selective migration time for DNC (*m/z* 303.0, 305 s) and HDP (*m/z* 125.1, 230 s) in the NIC sample suggests two independent species with the same migration behavior and respective MS response as the single compounds in DNC and HDP solutions. This leads to the conclusion that NIC undergoes dissociation in ACN based BGE into HDP and DNC, whereby DNC can be deprotonated in this medium.

3.1.2. *The effects of HDP and DNC on the analytical signal of NIC in DPV and CE-AD*

In view of the electrochemical activity of both NIC constituents, the contributions of HDP and DNC to the electroanalytical response of NIC were further investigated, aiming to enhance comprehension of its electrochemical oxidation on Pt UME. Hereinafter, CV was replaced by DPV to enhance the sensitivity and minimize background current.

The standard additions of DNC solution (20.0, 40.0, and 60.0 μM) were added to 50.0 μM NIC solution with the goal of evaluating the contribution of DNC to the electroanalytical response of NIC measured by CE-AD and DPV (Fig. 2a and b). In CE-AD, CAF (50 μM) was added to the solutions as an EOF marker. The electropherograms in Fig. 2 a demonstrate that the distinct peak of NIC at 365 s increases with increasing of DNC concentration, confirming that the DNC-related signal represents the analytical signal of NIC in CE-AD. Notably, this finding holds significant implications for practical application in real-world scenarios, as DNC functions as a specific biomarker for the detection of NIC residues in poultry tissues [27,67]. Additionally, this study illustrates the excellent reproducibility of the migration time of the analyte.

Concerning DPV determination, DNC additions to the NIC solution confirm the considerable electrochemical activity of DNC and its well-pronounced contribution to the overall oxidation signal of NIC, as illustrated in Fig. 2 b. This is evidenced by the clear growth of the NIC peak at 1.3 V, with the increase in DNC concentration while maintaining a constant NIC concentration. An additional experiment was conducted in this context, with the intention of investigating the role of HDP in NIC

Table 1
Results of CE-MS experiments of DNC, HDP, and NIC in positive ESI, *m/z* values taken from mass spectra in Fig. S2, Fig. S3 (supporting information), and migration times taken from Fig. S1.

tm	*m/z*	ESI	sample
230 s	125.1	$[M + H]^+$	HDP, NIC
305 s	303.0	$[M + H]^+$	DNC, NIC

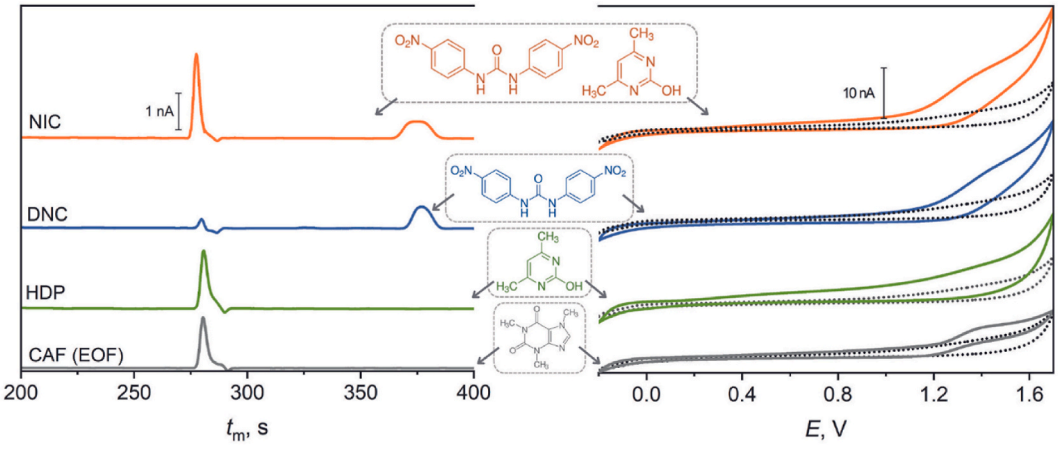

Fig. 1. CE-AD recordings (left) and CVs (right) of solutions NIC (orange), DNC (blue), HDP (green), and CAF (grey) in BGE on Pt UME ($C_{NIC} = C_{DNC} = C_{HDP} = C_{CAF} =$ 50.0 μM for CE-AD, $C_{NIC} = C_{DNC} = C_{HDP} = = C_{CAF} = 450.0$ μM for CV). CE parameters: separation voltage 20 kV, injection time 10 s, detection potential after HV correction 2.0 V. CV parameters: scan rate 100 mV s^{-1}, forward scan from −0.2 to 1.7 V and backward scan from 1.7 to −0.2 V. Black dots indicate CV of BGE. (For interpretation of the references to colour in this figure legend, the reader is referred to the Web version of this article.)

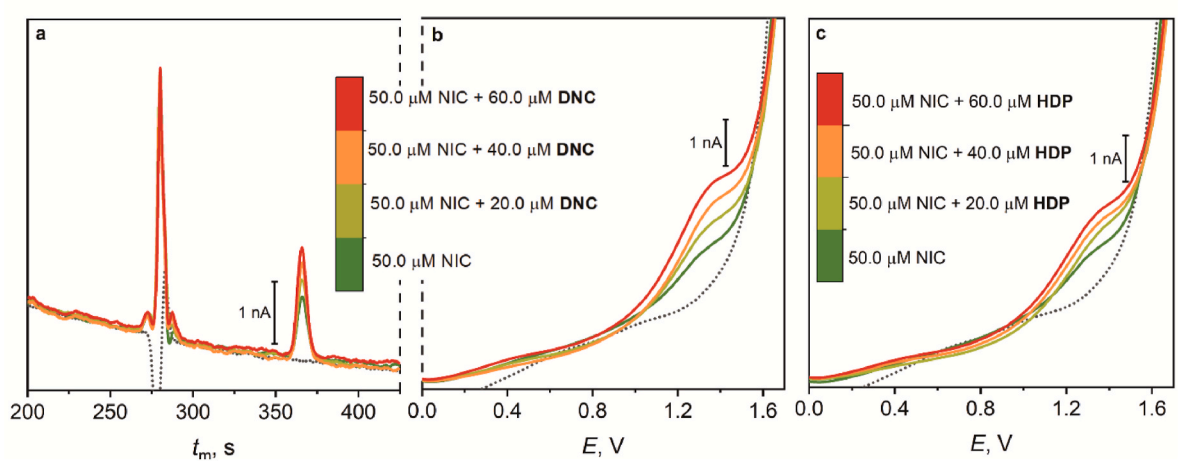

Fig. 2. CE-AD recordings (a) and DPVs (b, c) of 50.0 µM solutions NIC with standard additions of DNC (a, b) and HDP (c) solutions on Pt UME. CAF (50.0 µM) was added as an EOF marker. CE parameters: separation voltage 20 kV, injection time 10 s, detection potential after HV correction 2.0 V. DPV parameters: E_{pulse} = 100 mV, t_{pulse} = 100 ms, E_{step} = 10 mV, ν = 50 mV s^{-1}. Black dots indicate signal of BGE (10.0 mM ammonium acetate and 1.0 M acetic acid in ACN for CE-AD or 5.0 mM ammonium acetate and 0.5 M acetic acid in ACN for DPV).

oxidation signal. To achieve that, the standard additions of HDP solution (20.0, 40.0, and 60.0 µM) were added to 50.0 µM NIC solution in the identical manner as for DNC before. DPVs depicted in Fig. 2 c demonstrate the lower contribution of HDP to the NIC response, as well as less-pronounced electrochemical activity of HDP compared to DNC, which is consistent with the less distinct oxidation signal of HDP observed in CV (Fig. 1, right panel).

3.2. Investigation of NIC oxidation in acetonitrile based media on platinum electrodes by EC-CE-MS

EC-CE-MS was performed to investigate the oxidation processes of NIC in ACN based BGE during the CE-AD and DPV detection. In the EC-CE-MS experiments, Pt was used as a pseudo-reference electrode. For the investigation of electrochemical oxidation, 0.45 mM NIC in ACN based BGE was used. The electropherograms are shown in Fig. 3 a and Fig. 3 b. The *m/z* value for each species was taken from the respective mass spectrum in the supporting information (see Figs. S 5–7).

NIC was injected at open circuit potential (OCP) (Fig. 3 a) and at 2.5 V *vs.* Pt (Fig. 3 b). At OCP, the total ion electropherogram (TIE, grey) shows only one signal at 335 s, which corresponds to DNC *m/z* 301.0 ($[M - H]^-$, red) and a *m/z* 137.0 ESI fragment (black), displayed as selected ion electropherograms. The *m/z* 137.0 signal shows the highest intensity, leading to the conclusion that DNC is prone to fragmentation during the ESI process. There is no signal related to HDP observable, like in positive ESI (see Fig. 1S), suggesting that negative ESI is not suitable for HDP detection. The TIE of the injection at 2.5 V shows two additional signals at 270 s and 280 s, which could be associated with electrochemical DNC oxidation in NIC. Both product species show an ESI fragment with *m/z* 137.0, which corresponds to the same ESI fragment found in DNC (*m/z* 137.0). This fragment could be assigned to 4-nitroanline, which is an integral structural element of DNC. For further clarification, the migration behavior and ESI mass spectrometry pattern of 4-nitroaniline were investigated. A comparison with a 1 mM 4-nitroanilne standard (electropherograms Fig. 3 c) injected at OCP indicates that the fragment is related to the respective structural element in DNC and its final products P1 and P2 (see Fig. 3 a and mass spectra in Figs. S5–7). Additionally, P1 shows a signal for *m/z* 165.0 (see Fig. 3 a). A further comparison with the electropherograms of a 1 mM (4-nitrophenyl)formamide standard (see Fig. 3 d) suggests the cleavage of one C–N bond in the symmetrical DNC molecule during electrochemical oxidation at Pt electrodes in ACN based media, resulting in 4-nitroaniline and (4-nitro-phenyl)formamide as reaction product. We assume, that a number of associated redox processes in the ACN based BGE occur, resulting in the final reaction products P1 and P2, as shown in Scheme 1.

The measurements displayed in Fig. 3 a and Fig. 3 b were repeated with DNC solution (0.45 mM in ACN based BGE), leading to the same results (see Fig. S4).

3.3. Analytical performance of CE-AD and DPV for NIC determination

To estimate the basic analytical parameters of the proposed methods, the calibration dependencies were constructed for NIC concentrations in the range from 5.0 to 75.0 µM for DPV and CE-AD.

The electropherograms depicted in Fig. 4 a show a linear concentration dependency for concentrations from 5.0 to 75.0 µM. Based on these measurements, the LOD was 2.0 µM and LOQ was 6.6 µM.

For DPV, an electrochemical pretreatment of the Pt UME was applied for 10 s at 0.9 V in the analyzed solution to provide more stable and reproducible measurements (after this procedure, peak current was approximately 2.5 times higher (see Fig. S8) with a RSD of less than 4 % (n = 3) compared to recordings without incorporated pretreatment step). As can be seen in Fig. 4 b, the anodic peak current in DPV increases linearly with NIC concentration up to 75.0 µM without any variation of the peak potential (all measurements were performed in triplicate). The calculated LOD and LOQ values for DPV are 3.3 and 11.1 µM, respectively.

The linearity of calibration dependencies obtained by CE-AD and DPV is described in Eq. (1) and Eq. (2), respectively:

$$I_p\ (\text{nA}) = (0.035 \pm 0.0003)\ (\text{nA}/\mu\text{M}) \times C_{\text{NIC}}\ (\mu\text{M}) + (0 \pm 0.015)\ (\text{nA});\ R = 0.9959. \quad \text{(Eq. 1)}$$

$$I_p\ (\text{nA}) = (0.0063 \pm 0.0002)\ (\text{nA}/\mu\text{M}) \times C_{\text{NIC}}\ (\mu\text{M}) + (0.019 \pm 0.007)\ (\text{nA});\ R = 0.9983. \quad \text{(Eq. 2)}$$

Although higher concentrations of NIC were not measured due to its low solubility, the studied calibration range is suitable for monitoring NIC levels in therapeutic feed that contains the maximum allowed NIC content of 50 mg/kg, as regulated by EU legislation [68]. This range also effectively involves the analysis of contaminated feed with much lower NIC levels. Furthermore, the analysis of premix samples containing higher concentrations of NIC is feasible, as will be demonstrated in the subsequent section.

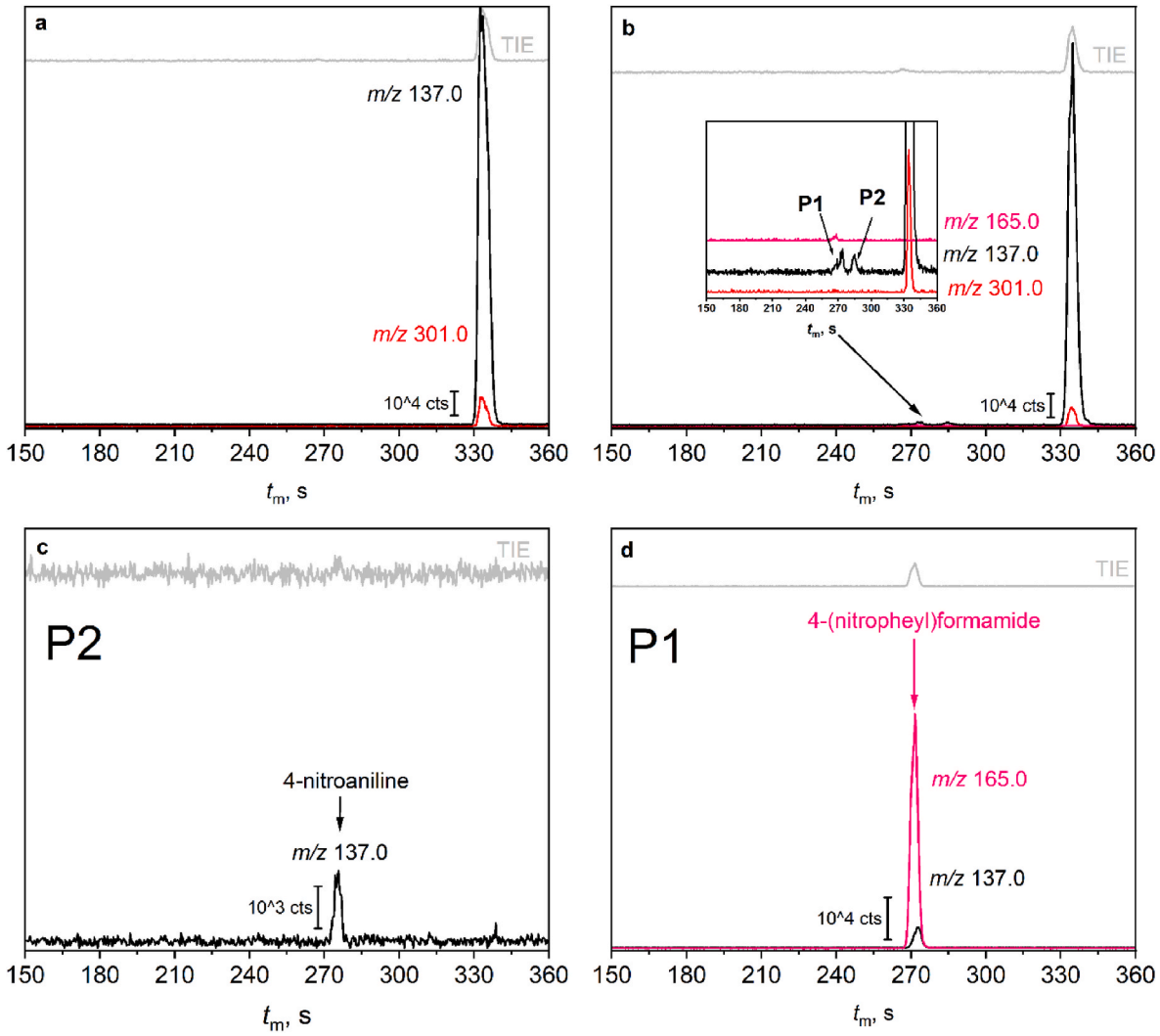

Fig. 3. EC-CE-MS recordings of 0.45 mM NIC, 1 mM (4-nitro-phenyl)formamide, and 1 mM 4-nitroaniline in ACN based BGE. (a) injection of NIC at open circuit; (b) injection of NIC at 2.5 V *vs.* Pt; (c) injection of 4-nitro-aniline at open circuit; (d) injection of (4-nitrophenyl)formamide at open circuit. Total ion electropherogram (TIE, grey) and extracted mass electropherograms (*m/z* 301.0 red, *m/z* 165.0 pink, *m/z* 137.0 black). Experimental conditions: Oxidation of sample for 300 s, followed by hydrodynamic injection for 60 s, separation voltage 20 kV, capillary length 50 cm, capillary inner diameter 75 μm. ESI-MS ion polarity mode: negative. (For interpretation of the references to colour in this figure legend, the reader is referred to the Web version of this article.)

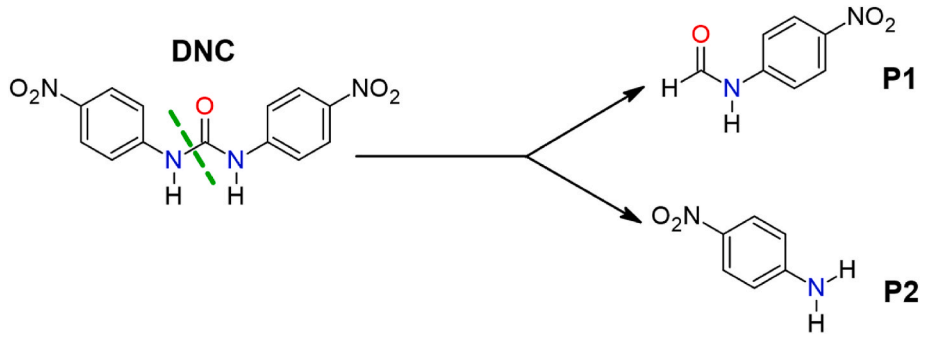

Scheme 1. Schematic representation of the final products formed according to the electrochemical conversion of DNC in NIC samples, structures of DNC, and reaction products P1 and P2. Possible cleavage site (green, dashed line) in the DNC molecule.

3.4. Determination of NIC in poultry feed samples

To confirm the practical applicability of the developed methods, real feed samples were analyzed by DPV and CE-AD under optimal conditions. Three feed samples of different nature with different NIC content were used for this purpose. Detailed information regarding the preparation of feed samples and their analysis is provided in Section 2.3.4.

The electropherograms shown in Fig. 5 a of the different feed samples show different amperometric signals in the migration windows for positively and negatively charged species after CE separation, for

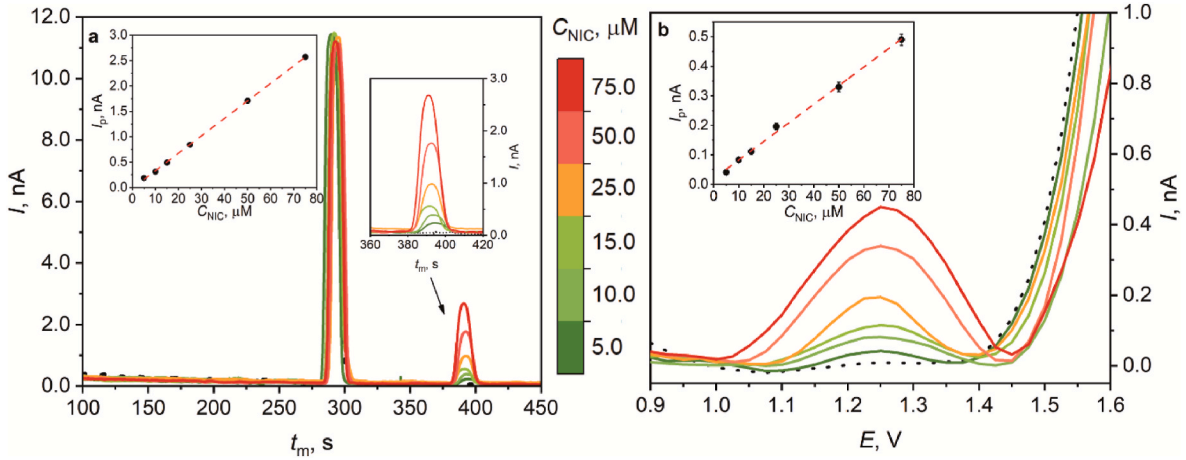

Fig. 4. CE-AD recordings (a) and baseline-corrected DPVs (b) of 5.0–75.0 μM NIC in ACN based BGE on Pt UME and the respective calibration dependencies in insets. CE parameters: separation voltage 20 kV, injection time 10 s, capillary length 60 cm, detection potential after HV correction 2.0 V. DPV parameters: E_{pulse} = 100 mV, t_{pulse} = 100 ms, E_{step} = 10 mV, ν = 50 mV s^{-1}. CAF (50 μM) was added as an EOF marker. Error bars correspond to the SDs of three parallel determinations.

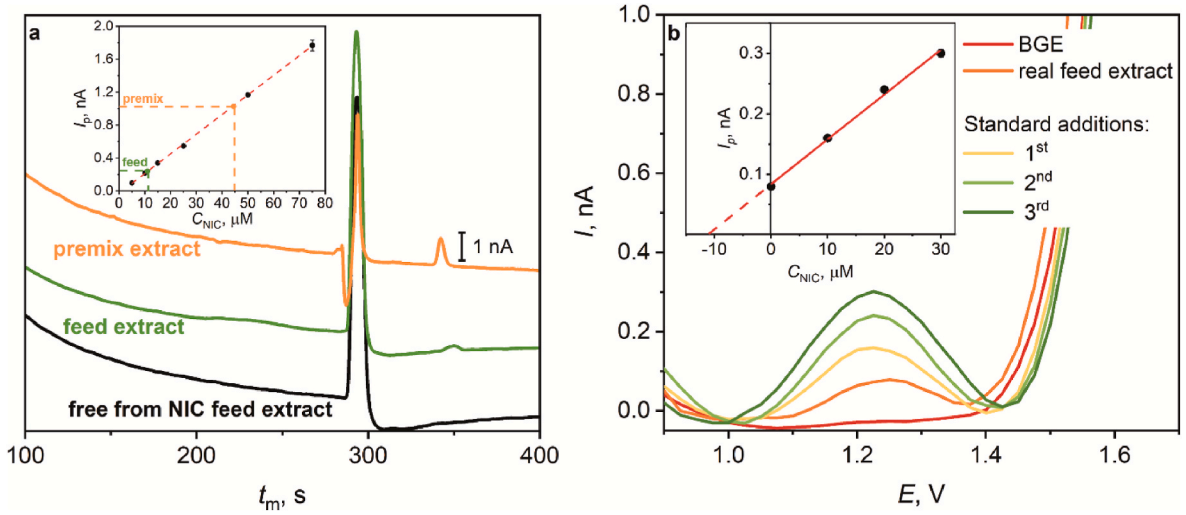

Fig. 5. NIC determination in real feed samples: CE-AD recordings of feed extract free from NIC (black), feed extract (green), and premix extract (orange). Respective external calibration dependence is shown in inset (a). Baseline-corrected DPVs recorded after electrochemical pretreatment at 0.9 V for 10 s using standard addition method for feed extract (three SA were 100 μL of 0.1 mM NIC stock solution) (b). CE parameters: separation voltage 20 kV, injection time 10 s, capillary length 60 cm, detection potential after HV correction 2.0 V. CAF (50 μM) was added as an EOF marker. DPV parameters: E_{pulse} = 100 mV, t_{pulse} = 100 ms, E_{step} = 10 mV, ν = 50 mV s^{-1}. Error bars correspond to the SDs of three parallel determinations. (For interpretation of the references to colour in this figure legend, the reader is referred to the Web version of this article.)

instance, 200 s for feed extract free from NIC and premix extract at 290 s. These signals indicate possible interfering substances that were successfully separated from the relevant NIC signal at 350 s.

For DPV analysis, two different approaches were employed for NIC determination: the standard additions (SA) method (via extrapolation) and matrix-fortified calibration (via interpolation). In preliminary studies, signals from each real sample were recorded from 0 to 1.7 V to check the entire potential window for the possible presence of additional peaks of other feed constituents. Since no other signals were observed in the whole potential window, all subsequent DPV measurements were performed with electrochemical pretreatment at 0.9 V for 10 s.

Fig. 5 b illustrates the model example of DPV analysis of feed using the SA method, where the extract was spiked by three SA, each 100 μL of 0.1 mM NIC stock (for analysis of premix by the identical method, see Fig. S9). Additionally, since DPV is more sensitive to matrix effects than CE-AD, the matrix effect was evaluated by comparing two calibration dependencies: one with fortified matrix extract in the range from 10.0 to 60.0 μM NIC and another without the matrix (using only standard solutions of NIC). Notably, a negligible signal was observed in the NIC-free feed at the potential related to NIC oxidation (1.2 V) (Fig. S9 a). This signal is consistent with CE-AD results (Fig. 5 a). However, the overlapping of the peaks of interferent and NIC precludes their evaluation. Importantly, the sensitivity of the matrix-fortified calibration did not significantly differ from calibration using standard NIC solutions, signifying that the proposed electroanalytical protocol did not suffer from any substantial matrix effect. LOD and LOQ values of this calibration dependence are 3.5 and 11.5 μM, respectively (Fig. S10 b). Subsequently, the analysis of NIC-containing feed and premix was performed using the matrix-fortified calibration. The concentrations of NIC found are shown in Fig. S10 b and Table 2.

Independently, these feed samples were analyzed by LC-MS/MS in National Reference Laboratory of Veterinary Drug Residues Control (State Scientific Research Control Institute of Veterinary Medicinal Products and Feed Additives, Lviv, Ukraine). These results served as a reference to compare the accuracy of our developed methods. The results obtained for NIC determination by DPV and CE-AD are summarized

Table 2
Results of analysis of the NIC-containing real feed samples on Pt UME by DPV and CE-AD ($n = 3$) and comparison with LC-MS/MS results.

Method of analysis	Method of determination	Found in feed, mg/kg	Found in premix, mg/kg
CE-AD	External calibration dependence	30.5 ± 1.5	14 184 ± 138
DPV	Matrix-fortified calibration	30.4 ± 1.2	15 568 ± 721
	Standard addition method	32.3 ± 1.9	15 828 ± 805
LC-MS/MS	Matrix-fortified calibration	31	15 783

in Table 2 and compared with LC-MS/MS results.

A comparative analysis of the two developed methods for NIC determination reveals that both CE-AD and DPV achieve comparable sensitivity, as evidenced by their similar LOD and LOQ. However, CE-AD demonstrates a clear advantage in terms of precision, outperforming DPV in this context. RSDs are lower than 5.0 % for both methods. On the other hand, DPV offers a significant advantage in terms of speed, with a single recording taking less than 30 s, compared to 420 s required for CE-AD analysis. In summary, while both methods exhibit comparable sensitivity, CE-AD emerges as a more precise technique with superior selectivity, while DPV offers a simple and fast determination of NIC. The choice between the two approaches will depend on the specific requirements of the analysis, such as the need for higher precision and selectivity or the necessity for rapid determination of NIC alone.

4. Conclusions

In this study, the electrochemical oxidation of the coccidiostat NIC is reported for the first time. Different electrochemical techniques were successfully employed to detect NIC oxidatively in non-aqueous media extracted from different types of poultry feed. While having the same electrochemical core characteristics, showing good reproducibility and high sensitivity with comparable LODs and LOQs in the lower μM range, DPV and CE-AD exhibit certain traits that can be beneficial in different situations. While DPV enabled an easy and fast analysis of each sample, only a more time-intensive CE-AD run was able to provide certainty about the presence of other electrochemically active substances in the poultry feed extracts. However, the results of both methods are in good agreement with an established LC-MS/MS method, proving that both methods are up to the task of NIC determination in poultry feed samples. As part of the holistic consideration of the two methods based on electrochemical oxidation at platinum electrodes, the electrode reaction was also investigated. It was found that the oxidative signal depends primarily on the DNC molecule contained in NIC. Additional CE-MS measurements also confirmed the dissociation of the NIC complex into its constituents, DNC and HDP, in ACN based media. By examining the electrode reaction using EC-CE-MS and comparing with standards, the cleavage of one C–N bond in DNC could be suggested, resulting in 4-nitroaniline and (4-nitrophenyl)formamide as final reaction products. This study shows that analytical electrochemistry is not a one-way street with only one solution to a problem. Although very similar in essence, the use of different electrochemical techniques in comparative studies can lead to an improved gain in information about various samples. Moreover, the newly developed CE-AD and DPV methods can contribute significantly to NIC monitoring and quality control in routine analysis due to their individual strengths to enable a safer application of NIC in livestock management.

CRediT authorship contribution statement

Sofiia Ivakh: Writing – review & editing, Writing – original draft, Visualization, Validation, Methodology, Investigation, Formal analysis, Data curation. **Martin Koall:** Writing – review & editing, Writing – original draft, Visualization, Validation, Methodology, Investigation, Formal analysis, Data curation. **Jiří Barek:** Writing – review & editing, Supervision, Resources, Project administration, Methodology, Funding acquisition, Conceptualization. **Frank-Michael Matysik:** Writing – review & editing, Supervision, Project administration, Methodology, Funding acquisition, Conceptualization.

Funding sources

This research was supported by the Grant Agency of Charles University (GAUK project 176424), Nadační fond of Faculty of Science of Charles University and Specific Charles University Research (SVV project 260690).

Declaration of competing interest

The authors declare that they have no known competing financial interests or personal relationships that could have appeared to influence the work reported in this paper.

Acknowledgments

The authors express their sincere gratitude to Dr. D. Yanovych, Dr. S. Plotytsia, Dr. M. Rydchuk, and Dr. D. Zasadna from National Laboratory of Veterinary Drug Residues Control (State Scientific Research Control Institute of Veterinary Medicinal Products and Feed Additives, Lviv, Ukraine) for their assistance in providing feed samples and conducting LC-MS/MS analysis.

Abbreviations

ACN acetonitrile;
BGE background electrolyte;
CAF caffeine;
CE-AD capillary electrophoresis with amperometric detection;
CE-MS capillary electrophoresis with mass spectrometry detection;
CV cyclic voltammetry (voltammogram);
DNC 4,4′-dinitrocarbanilide;
DPV differential pulse voltammetry (voltammogram);
EC-CE-MS coupling of pre-separation electrochemistry to capillary electrophoresis hyphenated to mass spectrometry;
EOF electroosmotic flow;
HDP 2-hydroxy-4,6-dimethylpyrimidine;
HV high voltage;
LC-MS/MS liquid chromatography – tandem mass spectrometry;
LOD limit of detection;
LOQ limit of quantification;
NIC nicarbazin;
OCP open circuit potential;
RSD relative standard deviation;
SA standard addition;
TIE total ion electropherogram;
UME ultramicroelectrode.

Appendix A. Supplementary data

Supplementary data to this article can be found online at https://doi.org/10.1016/j.talanta.2025.127729.

Data availability

Data will be made available on request.

References

[1] J. Wadhawan, E. Maisonhaute, Editorial overview: innovative methods in electrochemistry (2023): electrochemical techniques: smart approaches for timely problems, Curr. Opin. Electrochem. 43 (2024) 101426, https://doi.org/10.1016/j.coelec.2023.101426.

[2] K. Čokrtová, V. Mareš, T. Křížek, On-capillary fluorescent labeling of saccharides for capillary electrophoresis, Electrophoresis 44 (2023) 35–43, https://doi.org/10.1002/elps.202200136.

[3] A. Beutner, T. Herl, F.-M. Matysik, Selectivity enhancement in capillary electrophoresis by means of two-dimensional separation or dual detection concepts, Anal. Chim. Acta 1057 (2019) 18–35, https://doi.org/10.1016/j.aca.2018.11.042.

[4] Y. Wu, X. Wang, Z. Pang, J. Zhang, C. Zheng, Rapid and simultaneous analysis of monoiodoacetic acid and inorganic iodine in drinking water by capillary electrophoresis-inductively coupled plasma mass spectrometry, Microchem. J. 203 (2024) 110809, https://doi.org/10.1016/j.microc.2024.110809.

[5] Z. Wang, M. Li, S. Xu, L. Sun, L. Li, High-throughput relative quantification of fatty acids by 12-plex isobaric labeling and microchip capillary electrophoresis - mass spectrometry, Anal. Chim. Acta 1318 (2024) 342905, https://doi.org/10.1016/j.aca.2024.342905.

[6] A.-A. Peláez-Cid, S. Blasco-Sancho, F.-M. Matysik, Determination of textile dyes by means of non-aqueous capillary electrophoresis with electrochemical detection, Talanta 75 (2008) 1362–1368, https://doi.org/10.1016/j.talanta.2008.01.049.

[7] M. Koall, D. Böhm, T. Herl, F.-M. Matysik, Sensitive and selective determination of the neonicotinoid nitenpyram utilizing capillary electrophoresis hyphenated to amperometric detection/mass spectrometry, Electroanalysis 35 (2023) e202300238, https://doi.org/10.1002/elan.202300238.

[8] M. Baroch, H. Dejmková, F.-M. Matysik, Determination of trimetazidine in urine by capillary electrophoresis with amperometric detection, Monatsh. Chem. 154 (2023) 1013–1018, https://doi.org/10.1007/s00706-023-03083-2.

[9] A. Bard, L.R. Faulkner, Electrochemical Methods, Fundamentals and Applications, second ed., Wiley, 2001, 0-471-04372-9.

[10] J. Wang, Analytical Electrochemistry, fourth ed., Wiley, 2023, 978-1-119-78769-3.

[11] H. Bin Hamzah Hisham, A Study on the Estimating DPV Surface Coverages for Chemically Modified Electrodes, University of Southampton Institutional Repository, 2017. Doctoral Thesis, http://eprints.soton.ac.uk/id/eprint/416440.

[12] Á. Molina, E. Laborda, E.I. Rogers, F. Martínez-Ortiz, C. Serna, J.G. Limon-Petersen, N.V. Rees, R.G. Compton, Theoretical and experimental study of Differential Pulse Voltammetry at spherical electrodes: measuring diffusion coefficients and formal potentials, J. Electroanal. Chem. 634 (2009) 73–81, https://doi.org/10.1016/j.jelechem.2009.07.011.

[13] A. Dmukhailo, S. Tvorynska, L. Dubenska, Rapid and straightforward electrochemical approach for the determination of the toxic food azo dye tartrazine using sensors based on silver solid amalgam, J. Electroanal. Chem. 932 (2023) 117250, https://doi.org/10.1016/j.jelechem.2023.117250.

[14] T. Birhanzlová - Rumlová, J. Barek, J. Fischer, V. Vyskočil, Anodic differential pulse voltammetric determination of 2-nitrophenol at a non-traditional carbon film composite electrode, J. Electroanal. Chem. 877 (2020) 114510, https://doi.org/10.1016/j.jelechem.2020.114510.

[15] O. Sarakhman, L. Dubenska, Ľ. Švorc, First voltammetric behavior study of non-narcotic analgesic drug nefopam and its reliable determination on boron-doped diamond electrodes, J. Electroanal. Chem. 858 (2020) 113759, https://doi.org/10.1016/j.jelechem.2019.113759.

[16] A. Lytvynenko, S. Baluchová, J. Zima, J. Krůšek, K. Schwarzová-Pecková, Biofouling and performance of boron-doped diamond electrodes for detection of dopamine and serotonin in neuron cultivation media, Bioelectrochemistry 158 (2024) 108713, https://doi.org/10.1016/j.bioelechem.2024.108713.

[17] V. Hrdlička, J. Barek, T. Navrátil, Differential pulse voltammetric determination of homovanillic acid as a tumor biomarker in human urine after hollow fiber-based liquid-phase microextraction, Talanta 221 (2021) 121594, https://doi.org/10.1016/j.talanta.2020.121594.

[18] M. Aslan, A. Levent, Electrochemical investigation of the antimicrobial agent daptomycin utilizing disposable pencil graphite electrode and DNA interaction with green techniques, Microchem. J. 207 (2024) 112191, https://doi.org/10.1016/j.microc.2024.112191.

[19] M. Aslan, F. Aydin, A. Levent, Voltammetric studies and spectroscopic investigations of the interaction of an anticancer drug bevacizumab-DNA and analytical applications of disposable pencil graphite sensor, Talanta 265 (2023) 124823, https://doi.org/10.1016/j.talanta.2023.124893.

[20] R. Šelešovská, T. Navrátil, V. Hrdlička, P. Michniak, M. Hatala, M. Vojs, M. Marton, O. Matvieiev, L. Janíková, J. Chýlková, Novel screen-printed sensors with chemically deposited boron-doped diamond and their use for voltammetric determination of attention deficit hyperactivity disorder medication atomoxetine, Electrochim. Acta 403 (2022) 139642, https://doi.org/10.1016/j.electacta.2021.139642.

[21] D.M. Heard, A.J.J. Lennox, Electrode materials in modern organic electrochemistry, Angew. Chem. Int. Ed. 59 (2020) 18866–18884, https://doi.org/10.1002/anie.202005745.

[22] V. Briega-Martos, K. Stojanovski, M. Zlatar, C. Göllner, S. Cherevko, pH dependence of noble metals dissolution: platinum, Electrochim. Acta 501 (2024) 144793, https://doi.org/10.1016/j.electacta.2024.144793.

[23] K. Izutsu, History of the use of nonaqueous media in electrochemistry, J. Solid State Electrochem. 15 (2011) 1719–1731, https://doi.org/10.1007/s10008-010-1246-y.

[24] F.M. Matysik, Application of non-aqueous capillary electrophoresis with electrochemical detection to the determination of nicotine in tobacco, J. Chromatogr. A 853 (1999) 27–34, https://doi.org/10.1016/s0021-9673(99)00512-9.

[25] J.L. Miller, M.G. Khaledi, D. Shea, Separation of polycyclic aromatic hydrocarbons by nonaqueous capillary electrophoresis using charge-transfer complexation with planar organic cations, Anal. Chem. 69 (1997) 1223–1229, https://doi.org/10.1021/ac960734n.

[26] S.H. Hansen, J. Tjørnelund, I. Bjørnsdottir, Selectivity enhancement in capillary electrophoresis using non-aqueous media, TrAC, Trends Anal. Chem. 15 (1996) 175–180, https://doi.org/10.1016/0165-9936(96)00006-4.

[27] D.M. Bacila, V. Feddern, L.I. Mafra, G.N. Scheuermann, L. Molognoni, H. Daguer, Current research, regulation, risk, analytical methods and monitoring results for nicarbazin in chicken meat: a perspective review, Food Res. Int. 99 (2017) 31–40, https://doi.org/10.1016/j.foodres.2017.07.011.

[28] C.A. Yoder, L.A. Miller, K.S. Bynum, Comparison of nicarbazin absorption in chickens, mallards, and Canada geese, Poult. Sci. 84 (2005) 1491–1494, https://doi.org/10.1093/ps/84.9.1491.

[29] A.C. Cuckler, C.M. Malanga, A. J. Basso, R.C. O'Neill, Antiparasitic activity of substituted carbanilide complexes, Science 122 (n.d.) 244–245.

[30] L. Clarke, T.L. Fodey, S.R.H. Crooks, M. Moloney, J. O'Mahony, P. Delahaut, R. O'Kennedy, M. Danaher, A review of coccidiostats and the analysis of their residues in meat and other food, Meat Sci. 97 (2014) 358–374, https://doi.org/10.1016/j.meatsci.2014.01.004.

[31] C. Mesa-Pineda, J.L. Navarro-Ruíz, S. López-Osorio, J.J. Chaparro-Gutiérrez, L. M. Gómez-Osorio, Chicken coccidiosis: from the parasite lifecycle to control of the disease, Front. Vet. Sci. 8 (2021), https://doi.org/10.3389/fvets.2021.787653.

[32] Regulation (EC, No 1831/2003 of the European parlament anf of the council, Off. J. Eur. Union (2003). https://eur-lex.europa.eu/eli/reg/2003/1831/oj (accessed August 9, 2024).

[33] A review of coccidiostat residues in poultry, Safefood (n.d.). https://www.safefood.net/research-reports/coccidiostat-residues-poultry (accessed August 9, 2024).

[34] W.J. Blanchflower, P.J. Hughes, D.G. Kennedy, Determination of nicarbazin in eggs by liquid chromatography–atmospheric pressure chemical ionization mass spectrometry, J. AOAC Int. 80 (1997) 1177–1182, https://doi.org/10.1093/jaoac/80.6.1177.

[35] A. Cannavan, G. Ball, D.G. Kennedy, Determination of nicarbazin in feeds using liquid chromatography–electrospray mass spectrometry, Analyst 124 (1999) 1431–1434, https://doi.org/10.1039/A904557K.

[36] G. Stubbings, T. Bigwood, The development and validation of a multiclass liquid chromatography tandem mass spectrometry (LC–MS/MS) procedure for the determination of veterinary drug residues in animal tissue using a QuEChERS (QUick, Easy, CHeap, Effective, Rugged and Safe) approach, Anal. Chim. Acta 637 (2009) 68–78, https://doi.org/10.1016/j.aca.2009.01.029.

[37] M.R. Coleman, J.M. Rodewald, S.L. Brunelle, M. Nelson, L. Bailey, T.J. Burnett, Determination and confirmation of nicarbazin, measured as 4,4-dinitrocarbanilide (DNC), in chicken tissues by liquid chromatography with tandem mass spectrometry: first action 2013.07, J. AOAC Int. 97 (2014) 630–640, https://doi.org/10.5740/jaoacint.13-197.

[38] M. Cronly, P. Behan, B. Foley, E. Malone, P. Shearan, L. Regan, Determination of eleven coccidiostats in animal feed by liquid chromatography–tandem mass spectrometry at cross contamination levels, Anal. Chim. Acta 700 (2011) 26–33, https://doi.org/10.1016/j.aca.2010.11.001.

[39] J.L. Matus, J.O. Boison, A multi-residue method for 17 anticoccidial drugs and ractopamine in animal tissues by liquid chromatography-tandem mass spectrometry and time-of-flight mass spectrometry, Drug Test. Anal. 8 (2016) 465–476, https://doi.org/10.1002/dta.2019.

[40] L. Mortier, E. Daeseleire, C. Van Peteghem, Liquid chromatographic tandem mass spectrometric determination of five coccidiostats in poultry eggs and feed, J. Chromatogr. B 820 (2005) 261–270, https://doi.org/10.1016/j.jchromb.2005.04.016.

[41] O.W. Parks, Rapid procedure for determination of nicarbazin residues in chicken tissues, J. AOAC Int. 71 (1988) 778–780, https://doi.org/10.1093/jaoac/71.4.778.

[42] R. Draisci, L. Lucentini, P. Boria, C. Lucarelli, Micro high-performance liquid chromatography for the determination of nicarbazin in chicken tissues, eggs, poultry feed and litter, J. Chromatogr. A 697 (1995) 407–414, https://doi.org/10.1016/0021-9673(94)00960-H.

[43] S.-H. Chang, Y.-H. Lai, C.-N. Huang, G.-J. Peng, C.-D. Liao, Y.-M. Kao, S.-H. Tseng, D.-Y. Wang, Multi-residue analysis using liquid chromatography tandem mass spectrometry for detection of 20 coccidiostats in poultry, livestock, and aquatic tissues, J. Food Drug Anal. 27 (2019) 703–716, https://doi.org/10.1016/j.jfda.2019.02.004.

[44] M.M. De Zan, C.M. Teglia, J.C. Robles, H.C. Goicoechea, A novel ion-pairing chromatographic method for the simultaneous determination of both nicarbazin components in feed additives: chemometric tools for improving the optimization and validation, Talanta 85 (2011) 142–150, https://doi.org/10.1016/j.talanta.2011.03.043.

[45] E. Capurro, M. Danaher, A. Anastasio, M.L. Cortesi, M. O'Keeffe, Efficient HPLC method for the determination of nicarbazin, as dinitrocarbanilide in broiler liver, J. Chromatogr. B 822 (2005) 154–159, https://doi.org/10.1016/j.jchromb.2005.05.033.

[46] E. Protasiuk, M. Olejnik, T. Szprengier–Juszkiewicz, P. Jedziniak, J. Zmudzki, Determination of nicarbazin in animal feed by high-performance liquid chromatography with interlaboratory evaluation, Anal. Lett. 48 (2015) 2183–2194, https://doi.org/10.1080/00032719.2015.1025277.

[47] D.K. Matabudul, N.T. Crosby, S. Sumar, A new and rapid method for the determination of nicarbazin residues in poultry feed, eggs and muscle tissue using supercritical fluid extraction and high performance liquid chromatography, Analyst 124 (1999) 499–502, https://doi.org/10.1039/A808327D.
[48] R.S. Stahl, J.J. Johnston, High-performance liquid chromatography-based determination of nicarbazin excretion in waterfowl, J. Chromatogr. B 775 (2002) 103–108, https://doi.org/10.1016/S1570-0232(02)00165-4.
[49] J.A. Tarbin, G. Shearer, High-performance liquid chromatographic method for the determination of the dinitrocarbanilide component of nicarbazin in eggs with on-line clean-up, J. Chromatogr. B Biomed. Sci. Appl. 613 (1993) 354–358, https://doi.org/10.1016/0378-4347(93)80154-V.
[50] M.H. Vertommen, A. van der Laan, H.M. Veenendaal-Hesselman, High-performance liquid chromatographic screening method for low levels of nicarbazin in eggs with off-line cartridge sample clean-up, J. Chromatogr. A 481 (1989) 452–457, https://doi.org/10.1016/S0021-9673(01)96795-0.
[51] F. Barreto, C. Ribeiro, R.B. Hoff, T.D. Costa, A simple and high-throughput method for determination and confirmation of 14 coccidiostats in poultry muscle and eggs using liquid chromatography – quadrupole linear ion trap - tandem mass spectrometry (HPLC–QqLIT-MS/MS): validation according to European Union 2002/657/EC, Talanta 168 (2017) 43–51, https://doi.org/10.1016/j.talanta.2017.02.007.
[52] M. Rydchuk, S. Plotytsia, Z. Zasadna, D. Yanovych, Simple and efficient UPLC-ESI-MS/MS method for multi-residue analysis of 14 coccidiostatic agents in poultry liver and muscle tissues, Food Control 152 (2023) 109815, https://doi.org/10.1016/j.foodcont.2023.109815.
[53] M. Moloney, L. Clarke, J. O'Mahony, A. Gadaj, R. O'Kennedy, M. Danaher, Determination of 20 coccidiostats in egg and avian muscle tissue using ultra high performance liquid chromatography–tandem mass spectrometry, J. Chromatogr. A 1253 (2012) 94–104, https://doi.org/10.1016/j.chroma.2012.07.001.
[54] F. Kondo, E. Hamada, C.E. Tsai, S. Tateyama, K. Saitanu, A reverse-phase high-performance liquid chromatographic determination of nicarbazin residues in eggs - PubMed, Cytobios 76 (1993) 175–182. https://pubmed.ncbi.nlm.nih.gov/8181307/ (accessed August 9, 2024).
[55] R.C. Beier, L.H. Ripley, C.R. Young, C.M. Kaiser, Production, characterization, and cross-reactivity studies of monoclonal antibodies against the coccidiostat nicarbazin, J. Agric. Food Chem. 49 (2001) 4542–4552, https://doi.org/10.1021/jf010208j.
[56] A.-C. Huet, L. Mortier, E. Daeseleire, T. Fodey, C. Elliott, P. Delahaut, Screening for the coccidiostats halofuginone and nicarbazin in egg and chicken muscle: development of an ELISA, Food Addit. Contam. 22 (2005) 128–134, https://doi.org/10.1080/02652030500038041.
[57] L. Connolly, T.L. Fodey, S.R.H. Crooks, P. Delahaut, C.T. Elliott, The production and characterisation of dinitrocarbanilide antibodies raised using antigen mimics, J. Immunol. Methods 264 (2002) 45–51, https://doi.org/10.1016/S0022-1759(02)00040-6.
[58] B. McCarney, I.M. Traynor, T.L. Fodey, S.R.H. Crooks, C.T. Elliott, Surface plasmon resonance biosensor screening of poultry liver and eggs for nicarbazin residues, Anal. Chim. Acta 483 (2003) 165–169, https://doi.org/10.1016/S0003-2670(02)01470-8.
[59] K. Campbell, T. Fodey, J. Flint, C. Danks, M. Danaher, M. O'Keeffe, D.G. Kennedy, C. Elliott, Development and validation of a lateral flow device for the detection of nicarbazin contamination in poultry feeds, J. Agric. Food Chem. 55 (2007) 2497–2503, https://doi.org/10.1021/jf062811d.
[60] R.F. Michielli, G.V. Downing, Differential pulse polarographic determination of nicarbazin in chicken tissue, J. Agric. Food Chem. 22 (1974).
[61] G. Knupp, G. Bugl-Kreickmann, C. Commichau, T. Schmidt, H. Biining-Pfaue, Zur Bestimmung des Coccidiostaticums Nicarbazin in tierischem Gewebe und im Ei, Z. Lebensm. Unters. Forsch. 185 (1987) 472–476.
[62] J. Wood, G. Downing, Modified pulse polarographic determination of nicarbazin in chicken tissue at the 0.1-ppm level, J. Agric. Food Chem. 28 (1980) 452–454.
[63] C. Lema, A. Álvarez-Lueje, R. Moscoso, J.A. Squella, Electrochemical nicarbazin analysis: rapid determination on bucky paper disks constructed from MWCNT, J. Electrochem. Soc. 171 (2024) 066503, https://doi.org/10.1149/1945-7111/ad541a.
[64] M. Akilarasan, S. Kogularasu, S.-M. Chen, M. Govindasamy, T.-W. Chen, M.A. Ali, F.M.A. Al-Hemaid, M.S. Elshikh, M.A. Farah, A Green approach to the synthesis of well-structured prussian blue cubes for the effective electrocatalytic reduction of antiprotozoal agent coccidiostat nicarbazin, Electroanalysis 30 (2018) 1669–1677, https://doi.org/10.1002/elan.201700750.
[65] R. Schmid, S. Heuckeroth, A. Korf, A. Smirnov, O. Myers, T.S. Dyrlund, R. Bushuiev, K.J. Murray, N. Hoffmann, M. Lu, A. Sarvepalli, Z. Zhang, M. Fleischauer, K. Dührkop, M. Wesner, S.J. Hoogstra, E. Rudt, O. Mokshyna, C. Brungs, K. Ponomarov, L. Mutabdžija, T. Damiani, C.J. Pudney, M. Earll, P. O. Helmer, T.R. Fallon, T. Schulze, A. Rivas-Ubach, A. Bilbao, H. Richter, L.-F. Nothias, M. Wang, M. Orešič, J.-K. Weng, S. Böcker, A. Jeibmann, H. Hayen, U. Karst, P.C. Dorrestein, D. Petras, X. Du, T. Pluskal, Integrative analysis of multimodal mass spectrometry data in MZmine 3, Nat. Biotechnol. 41 (2023) 447–449, https://doi.org/10.1038/s41587-023-01690-2.
[66] F.-M. Matysik, Experimental characterization of end-column electrochemical detection in conjunction with non-aqueous capillary electrophoresis, Anal. Chem. 72 (2000) 2581–2586, https://doi.org/10.1021/ac9913326x.
[67] M. O'Keeffe, E. Capurro, M. Danaher, K. Campbell, C.T. Elliott, Investigation of the causes for the occurrence of residues of the anticoccidial feed additive nicarbazin in commercial poultry, Food Addit. Contam. 24 (2007) 923–934, https://doi.org/10.1080/02652030701258778.
[68] Commission Regulation (EU), No 37/2010 of 22 December 2009 on pharmacologically active substances and their classification regarding maximum residue limits in foodstuffs of animal origin (Text with EEA relevance). http://data.europa.eu/eli/reg/2010/37(1)/oj/eng, 2009. (Accessed 31 July 2024).